

Finite-temperature signatures of gap anisotropy in optical conductivity of ferropnictides

E. Schachinger^{1,*} and J. P. Carbotte^{2,3}¹*Institute of Theoretical and Computational Physics, Graz University of Technology, A-8010 Graz, Austria*²*Department of Physics and Astronomy, McMaster University, Hamilton, Ontario, Canada N1G 2W1*³*The Canadian Institute for Advanced Research, Toronto, Ontario, Canada M5G 1Z8*

(Received 24 February 2011; revised manuscript received 29 September 2011; published 17 October 2011)

The low-temperature optical conductivity in the superconducting state of the ferropnictides shows increased absorption at low energies not expected for an isotropic s -wave gap. This may indicate that the gap on one or more of the several bands involved is quite anisotropic. A possible candidate is the gap on the electron pocket at the M point in the Brillouin zone. We calculate the optical response of an extended s -wave superconductor with emphasis on its temperature evolution. An aim is to study the difference in signatures, both in temperature and frequency, expected in the crossover region between a gap with nodes and that with a small gap. Results are also presented for a two-band case with microscopic parameters chosen specific to the ferropnictides. We add their respective conductivities and, thus, neglect any interband contributions.

DOI: [10.1103/PhysRevB.84.134522](https://doi.org/10.1103/PhysRevB.84.134522)

PACS number(s): 74.25.N-, 74.20.Rp, 74.25.F-, 74.70.-b

I. INTRODUCTION

Superconductivity discovered in the FeAs family^{1,2} can have a critical temperature T_c up to ~ 55 K (Refs. 3 and 4). Only the cuprates have higher values. The parent compound can be doped, both with electrons as in $\text{BaFe}_{2-x}\text{Co}_x\text{As}_2$ (Ref. 5) or with holes as in $\text{Ba}_{1-x}\text{K}_x\text{Fe}_2\text{As}_2$ (Ref. 6). Band-structure calculations^{7,8} have shown that these systems represent an entire new class of multiband superconductors, but with a nonphonon mechanism⁹ in contrast to the well-known two-band case of MgB_2 (Ref. 10), which is believed to be electron-phonon driven.¹¹⁻¹³ The relatively high value of $T_c \sim 40$ K in those materials is traced not so much to its two-band nature, but to a relatively modest coupling to high-energy phonon modes. While the ferropnictides have more bands, a minimal model includes two bands, an electron band centered on the M point in the Brillouin zone and a hole band at point Γ , both with superconducting gap functions (Δ) having s -wave symmetry, but with a possible sign change in Δ between the two, the so-called s^\pm -symmetry state.^{8,14} The gap on the electron pocket could have extended s -wave character rather than be isotropic.¹⁵ Anisotropic s -wave gaps are in no way unusual. Even in conventional metals such as Al (Refs. 16 and 17), Pb (Ref. 18), and Nb (Ref. 19), the gap has been found to vary greatly on the Fermi surface, although there is no evidence for nodes in these systems. This means that when impurity scattering is increased, anisotropy in the superconducting gap washes out, but T_c remains finite as does the average gap value in contrast to d -wave symmetry where impurities can drive the critical temperature to zero very much in the same way as paramagnetic impurities do in isotropic s -wave superconductors.^{20,21} Other complications beyond isotropic s -wave Bardeen-Cooper-Schrieffer (BCS) theory have been considered in conventional superconductors, such as energy dependence in the electronic density of states,²²⁻²⁵ retardation effects due to the inelastic scattering,²⁶⁻²⁸ and related strong-coupling corrections.²⁹ These have not yet been found to be essential in discussions of the optical conductivity in the superconducting state in the ferropnictides beyond including an appropriate non-BCS value for the ratio of twice the superconducting gap to critical temperature. This procedure

has been found to simulate well strong-coupling effects in the work of Padamsee *et al.*³⁰ An important issue, however, has centered on whether the extended s -wave gap could have nodes³¹⁻³⁴ or, possibly, that there is a small gap everywhere on the electron Fermi surface, perhaps due to impurities.³⁵ Direct experimental information on band structure is available from angular resolved photoemission spectroscopy³⁶⁻⁴² (ARPES) and these studies so far favor an isotropic s -wave gap, but with different size on the various bands observed. However, different experimental probes give different results.

In both hole-doped $\text{Ba}_{1-x}\text{K}_x\text{Fe}_2\text{As}_2$ (Ref. 43) and electron-doped $\text{Ba}(\text{Fe}_{1-x}\text{Co}_x)_2\text{As}_2$ (Ref. 44) compounds, low-temperature thermal conductivity measurements indicate that the residual linear term corresponding to the universal limit is negligible, indicating that the gap does not have nodes. For $\text{Ba}_{1-x}\text{K}_x\text{Fe}_2\text{As}_2$, however, the application of a small magnetic field is found to induce a linear in temperature term.⁴³ This indicates that the minimum gap must be very small on at least one of the several bands involved. Data on the temperature dependence of the London penetration depth in $\text{Ba}_{1-x}\text{K}_x\text{Fe}_2\text{As}_2$ by Hashimoto *et al.*⁴⁵ indicate an exponentially activated temperature dependence at small T , which is not consistent with nodes in one of the gaps. On the other hand, a detailed analysis by Schachinger and Carbotte⁴⁶ of the microwave data on the same sample giving the real part of the optical conductivity at $\nu = 28$ GHz shows that it can be most naturally understood if there are nodes in the gap, although small minimum gaps can not be entirely ruled out. Nodes are also more consistent with separate penetration depth data by Martin *et al.*⁴⁷ on a closely related sample of $\text{Ba}_{1-x}\text{K}_x\text{Fe}_2\text{As}_2$. A very recent microwave measurement of the temperature dependence of the superfluid density in both $\text{Ba}_{0.72}\text{K}_{0.28}\text{Fe}_2\text{As}_2$ with $T_c \sim 30$ K and $\text{Ba}(\text{Fe}_{0.92}\text{Co}_{0.08})_2\text{As}_2$ with $T_c \sim 20$ K has found a power law for renormalized London penetration depth $\lambda_L^2(0)/\lambda_L^2(T) \sim T^n$ with $n \sim 2.5$ consistent with nodes.⁴⁸ On the other hand, Raman scattering data on $\text{Ba}(\text{Fe}_{1-x}\text{Co}_x)_2\text{As}_2$ by Muschler *et al.*⁴⁹ give spectroscopic evidence for nodes in the B_{2g} response of $\text{Ba}(\text{Fe}_{0.939}\text{Co}_{0.061})_2\text{As}_2$ with $T_c = 24$ K. For a slightly higher doping $\text{Ba}(\text{Fe}_{0.915}\text{Co}_{0.085})_2\text{As}_2$ with T_c reduced to 22 K, a small gap is seen to develop in the Raman

response, which becomes zero below a finite $\omega \sim 10 \text{ cm}^{-1}$ for $T = 8 \text{ K}$. The authors note that the residual scattering in their sample is of the same order of magnitude as is the gap. In this case, disorder can open up a finite gap due to washing out of anisotropy.³⁵

The optical conductivity of ferropnictides has been the subject of considerable activity, including measurements by Yang *et al.*⁵⁰ and Wu *et al.*⁵¹ both in Co-doped samples. These works are oriented more directly toward extracting information on the pairing interaction and involve the use of Eliashberg (strong-coupling) equations rather than BCS. A common conclusion of both studies is that spin fluctuations may play an important role in the glue causing condensation into a superfluid. The need for an Eliashberg approach has also been pointed out by other works.^{52,53} Other studies have been more directly aimed toward the superconducting state and gap symmetry and usually involve a BCS approach. The work of Wu *et al.*⁵⁴ is based on data by Barišić *et al.*⁵⁵ and Wu *et al.*⁵⁶ These authors conclude that the gap on the electron pocket at the M point in the Brillouin zone is large, of order 7.5 meV for their sample of $\text{Ba}(\text{Fe}_{0.92}\text{Co}_{0.08})_2\text{As}_2$ and the gap on the hole pocket at point Γ is of order 2.5 meV. For a second sample $\text{Ba}(\text{Fe}_{0.95}\text{Ni}_{0.05})_2\text{As}_2$, the gaps are 7 and 2.3 meV, respectively. Assuming the gap at the M point to be very anisotropic provides a natural explanation of the data, but the authors can not determine for sure whether there is a small optical gap or nodes. Such a small optical gap Δ_{qp}^0 is a region of zero absorption in the real part of the optical conductivity observed at very low temperatures. It will be twice the value of the gap Δ_{qp}^0 in the quasiparticle excitation spectrum (or in the quasiparticle density of states) on the Fermi surface induced by superconductivity.

Lobo *et al.*⁵⁷ provide a very different method of analysis of data in $\text{Ba}(\text{Fe}_{0.92}\text{Ni}_{0.08})_2\text{As}_2$. They find that it can not be fit within the s -wave Mattis-Bardeen description,⁵⁸ and an additional temperature-independent Drude form is needed. This provides evidence for additional low-frequency absorption beyond that in an isotropic s -wave superconductor, confirming the conclusion of Wu *et al.*⁵⁴ A similar conclusion is also made in the work of van Heumen *et al.*⁵⁹ with the difference that the extra low-energy absorption is assigned to some interband transitions. Other data that are consistent with increased low-energy absorption are THz measurements by Fischer *et al.*⁶⁰ On the other hand, data by Tu *et al.*⁶¹ can be understood with two isotropic gaps, one with $\Delta = 3.1 \text{ meV}$, the other with 7.4 meV for their $\text{BaFe}_{1.85}\text{Co}_{0.15}\text{As}_2$ sample with $T_c = 25 \text{ K}$. Nakajima *et al.*⁶² studied two samples of $\text{Ba}(\text{Fe}_{1-x}\text{Co}_x)_2\text{As}_2$ with $x = 0.06$ and 0.08 and found almost unit reflectivity below 80 and 50 cm^{-1} , respectively. In $\text{BaFe}_{1.87}\text{Co}_{0.13}\text{As}_2$ with $T_c = 24.5 \text{ K}$, Kim *et al.*⁶³ find a fit with three isotropic gaps of values $2\Delta/(k_B T_c) = 3.1, 4.7, \text{ and } 9.2$.

It is clear from this brief review of optical data that one can not yet conclude with certainty whether or not the superconducting gap on some of the several bands involved is anisotropic with a very small minimum effective gap or, perhaps, it has a node. To aid in the interpretation of existing data as well as provide guidance as to which feature of the optical conductivity and related optical quantities might fruitfully be focused on, we present results of calculations for an extended s -wave gap that focus on the frequency

dependence of the real part of the optical conductivity⁶⁴ at small energies ν and also on its temperature dependence. Finite-temperature effects could mask the existence of a small optical gap, which can only be detected at very low temperatures. An important feature of the work rests in a comparative study of the optical response of a sample with a small optical gap with another identical one, except that it just falls on the other side of the crossover point between a small gap and a node. While most of the work presented involves a single band, we also consider explicitly a two-band case. To do so, we simply add the conductivities for two bands properly weighted by their optical strength. This procedure assumes that, as a first approximation, interband effects are not large. Optical data for energies below twice the gap are most important in determining gap anisotropy. In this energy region, data by Charnukha *et al.*⁵³ on $\text{Ba}_{0.68}\text{K}_{0.32}\text{Fe}_2\text{As}_2$ and van Heumen *et al.*⁵⁹ for $\text{BaFe}_{2-x}\text{Co}_x\text{As}_2$ with $x = 0.14$ show that interband contributions are indeed small.

In Sec. II, we present the required formalism including the Kubo formula for the current-current correlation function of an extended s -wave superconductor and equations for the modification of the superconducting gap function when impurities are present. Impurities will not change the value of Δ_{qp}^0 or T_c in the isotropic case, but when there is anisotropy, impurities will wash it out progressively and Δ_{qp}^0 takes on its average value in the limit when the impurity scattering rate becomes much larger than the superconducting gap amplitude. Section III contains our numerical results. Much of the work involves a detailed look at the case of a single band with a highly anisotropic s -wave gap, including nodes possibly lifted by impurity scattering. These results are an essential preliminary step to a more specific discussion of the two-band case needed to describe ferropnictides. We summarize and make conclusions in Sec. IV.

II. FORMALISM

Fundamental to this work is the Kubo formula for the ac optical conductivity $\sigma(T, \nu)$ as a function of temperature T and photon energy ν . The conductivity tensor $\sigma_{jk}(\nu)$ can be written as^{46,64–68}

$$\sigma_{jk}(\nu) = \frac{i}{\nu} \Pi_{jk}(i\nu_n \rightarrow \nu + i0^+), \quad (1)$$

where the analytic continuation from the imaginary boson Matsubara frequencies $i\nu_n$ ($\nu_n = 2n\pi T$, $n = 0, \pm 1, \pm 2, \dots$) is taken to the real frequency axis $i\nu_n \rightarrow \nu + i0^+$. A standard approximation to $\Pi_{jk}(i\nu_n)$ in which vertex corrections for the electromagnetic interaction are neglected gives

$$\begin{aligned} \Pi_{jk}(i\nu_n) = & \frac{2T}{N} \sum_{m, \mathbf{p}} \text{Tr}\{e v_j(\mathbf{p}) G(\mathbf{p}, i\nu_n + i\omega_m) \\ & \times G(\mathbf{p}, i\omega_m) e v_k(\mathbf{p})\}, \end{aligned} \quad (2)$$

where $v_i(\mathbf{p})$ is the i th component of the Fermi velocity, $G(\mathbf{p}, i\omega_m)$ is the electron Green's function in the 2×2 Nambu notation, and $\text{Tr}\{\dots\}$ is the trace. In terms of the Matsubara

pairing energy $\tilde{\Delta}_{\mathbf{p}}(i\omega_m)$ and the renormalized Matsubara frequencies $\tilde{\omega}_{\mathbf{p}}(i\omega_m)$, the Green's function has the form

$$G(\mathbf{p}, i\omega_m) = \frac{\tilde{\omega}_{\mathbf{p}}(i\omega_m)\tau_0 + \epsilon_{\mathbf{p}}\tau_3 + \tilde{\Delta}_{\mathbf{p}}(i\omega_m)\tau_1}{\tilde{\omega}_{\mathbf{p}}^2(i\omega_m) - \epsilon_{\mathbf{p}}^2 - \tilde{\Delta}_{\mathbf{p}}^2(i\omega_m)}, \quad (3)$$

where τ_0 , τ_1 , and τ_3 are Pauli matrices and $\epsilon_{\mathbf{p}}$ is the electron dispersion. To get $\Pi_{jk}(i\nu_n)$ on the real frequency axis, we need to use the spectral representation of the Green's function. We obtain

$$\begin{aligned} \Pi_{jk}(\omega + i\delta) = & \left\langle 2e^2 N(0)v_j(\mathbf{p})v_k(\mathbf{p})\text{Tr} \left\{ \int d\epsilon \int d\Omega \right. \right. \\ & \times f(\Omega) \frac{-1}{\pi} \text{Im}G(\mathbf{p}, \Omega + i\delta)[G(\mathbf{p}, \Omega + \omega + i\delta) \\ & \left. \left. - G(\mathbf{p}, \Omega - \omega - i\delta)] \right\} \right\rangle_{\mathbf{p}}, \quad (4) \end{aligned}$$

with

$$G(\mathbf{p}, \omega + i\delta) = \frac{\tilde{\omega}_{\mathbf{p}}(\omega + i\delta)\tau_0 + \epsilon_{\mathbf{p}}\tau_3 + \tilde{\Delta}_{\mathbf{p}}(\omega + i\delta)\tau_1}{\tilde{\omega}_{\mathbf{p}}^2(\omega + i\delta) - \epsilon_{\mathbf{p}}^2 - \tilde{\Delta}_{\mathbf{p}}^2(\omega + i\delta)}. \quad (5)$$

Here, $f(\omega)$ is the fermionic thermal factor, $N(0)$ is the electronic density of states at the Fermi level, and $\langle \dots \rangle_{\mathbf{p}}$ indicates the average over the angle of \mathbf{p} . It has been assumed that the density of states factor $N(\epsilon)$ does not vary much over the energy range of importance for the energy integral in Eq. (4) and, thus, was taken out of the integral at its Fermi surface value $N(0)$. We also approximate the various bands by free electron bands and, consequently, the product $N(0)v_j(\mathbf{p})$ in Eq. (4) combines to $\Omega_p^2/(4\pi)$ in Eq. (6) with Ω_p the plasma frequency.

For a superconductor with anisotropic superconducting gap function $\Delta(\nu, \phi)$ on a cylindrical Fermi surface with polar angle ϕ , $\sigma(T, \nu)$ takes after considerable algebra the form^{46,64-68}

$$\sigma(T, \nu) = \frac{\Omega_p^2}{4\pi} \frac{i}{\nu} \left\langle \int_0^\infty d\omega \tanh\left(\frac{\beta\omega}{2}\right) [J(\omega, \nu) - J(-\omega, \nu)] \right\rangle_{\phi}, \quad (6)$$

where the bracket $\langle \dots \rangle_{\phi}$ indicates an average over ϕ and β is the inverse temperature $(k_B T)^{-1}$ with k_B the Boltzmann constant. The function $J(\omega, \nu)$ is given by

$$2J(\omega, \nu) = \frac{1 - N(\omega, \phi)N(\omega + \nu, \phi) - P(\omega, \phi)P(\omega + \nu, \phi)}{E(\omega, \phi) + E(\omega + \nu, \phi)} \quad (7)$$

$$+ \frac{1 + N^*(\omega, \phi)N(\omega + \nu, \phi) + P^*(\omega, \phi)P(\omega + \nu, \phi)}{E^*(\omega, \phi) - E(\omega + \nu, \phi)}, \quad (8)$$

with \star indicating the complex conjugate. Here,

$$E(\omega, \phi) = \sqrt{\tilde{\omega}^2(\omega + i0^+) - \tilde{\Delta}^2(\omega + i0^+, \phi)}, \quad (9a)$$

$$N(\omega, \phi) = \tilde{\omega}(\omega + i0^+)/E(\omega, \phi), \quad (9b)$$

$$P(\omega, \phi) = \tilde{\Delta}(\omega + i0^+, \theta)/E(\omega, \phi). \quad (9c)$$

As here, most discussions of the optical conductivity in the superconducting state neglect vertex corrections, which are not expected to change our results qualitatively and can be

incorporated mainly through changes of the scattering rate introduced below from its quasiparticle value to an appropriate transport version. For an extended s -wave gap, impurity scattering can change the value of the renormalized gap function $\tilde{\Delta}(\nu, \phi)$ as well as the renormalized quasiparticle frequency $\tilde{\omega}(\omega) = \omega - \Sigma_{qp}(\omega)$ with $\Sigma_{qp}(\omega)$ the quasiparticle self-energy. For the elastic quasiparticle scattering rate $\tau_{qp}^{-1} = \pi t^+$ in the Born approximation^{26,27} (with the corresponding optical scattering rate $\tau_{op}^{-1} = 2\tau_{qp}^{-1}$), we have

$$\tilde{\omega}(\omega + i0^+) = \omega + i\pi t^+ \langle N(\omega, \phi) \rangle_{\phi}, \quad (10a)$$

$$\begin{aligned} \tilde{\Delta}(\omega + i0^+, \phi) = & \alpha \Delta_0 + i\pi t^+ \langle P(\omega, \phi) \rangle_{\phi} \\ & + \sqrt{1 - \alpha^2} \Delta_0 \sqrt{2} \cos(2\phi), \quad (10b) \end{aligned}$$

with Δ_0 the superconducting gap amplitude. For simplicity, we present results here only for Born impurity scattering. This is sufficient for a first qualitative discussion of the physics involved. More complicated forms as described by Schürer *et al.*⁶⁵ could easily be introduced if data should indicate the need to do so. These equations need to be iterated, and the gap function $\tilde{\Delta}(\omega, \phi)$ will, in general, have both a real and imaginary part as is very familiar in Eliashberg theory,^{28,29} which includes inelastic scattering and so-called strong-coupling corrections. In the pure case with $t^+ = 0$, $\tilde{\Delta}(\omega + i0^+, \phi)$ reduces to a real function independent of frequency ω and has the form $\alpha \Delta_0 + \sqrt{1 - \alpha^2} \Delta_0 \sqrt{2} \cos(2\phi)$, which is the sum of an isotropic s -wave and an extended s -wave piece referred to a coordinate system centered on the M point in the Brillouin zone. As described by Chubukov *et al.*¹⁵ the gap function on this pocket could be anisotropic, while the gap function on the hole pocket centered about the Γ point is assumed to be isotropic s wave (i.e., $\alpha = 1$), but carrying the opposite sign amplitude to that on the electronic band, which establishes the so-called s^{\pm} -symmetry state. Anisotropic gap functions are well known even in conventional superconductors.¹⁶⁻¹⁹ Note that the gap amplitude Δ_0 is equal to the root-mean-square gap amplitude of the pure crystal ($t^+ = 0$). The parameter $\alpha = 1$ gives the pure isotropic case and $\alpha = 0$ the pure anisotropic case with nodes in the extended s -wave gap function on the electron pocket and averaging to zero on this Fermi surface. A node exists in the pure crystal superconducting gap function for $\alpha \leq \alpha_c = \sqrt{2/3}$. Throughout the paper, the anisotropy parameter $x = \alpha/(\alpha + \sqrt{1 - \alpha^2})$ is used instead of α . It has the critical value of $x = x_c = 0.59$, and it has the advantage that x multiplied by 100 gives the percentage of the s -wave component to the gap function. (The parameter α is related to x via $\alpha = x/\sqrt{1 - 2x + 2x^2}$.) In the anisotropic case for $\alpha > \sqrt{2/3}$, one must not confuse the superconducting gap amplitude Δ_0 in Eqs. (10) with the finite minimum gap Δ_{qp}^0 on the Fermi surface for quasiparticle excitation. This is the gap that opens in the quasiparticle density of states (DOS) and it also provides an optical gap $\Delta_{op}^0 = 2\Delta_{qp}^0$. Even for $\alpha < \sqrt{2/3}$, when there are nodes in the case of a pure crystal, these nodes can be lifted when impurity scattering is introduced and is sufficiently large to wash out the anisotropy enough that a gap Δ_{qp}^0 is generated in the quasiparticle excitation spectrum. As elastic impurity scattering increases, momentum no longer remains a good quantum number and each electron samples

many values of the superconducting gap function as the system moves toward isotropy at every point of the Fermi surface.

The parameters of the model are therefore Ω_p , α or x , Δ_0 , and t^+ . In what follows, we will present results for the real part of the optical conductivity $\sigma_1(T, \nu)$ versus photon energy for several values of temperature T . We will also consider the reflectance $r(T, \nu)$ as this is the quantity that is often directly measured in optics. It is related to the optical conductivity through the dielectric function

$$\epsilon(T, \nu) = \epsilon_\infty + i \frac{4\pi}{\nu} \sigma(T, \nu), \quad (11)$$

with

$$r(T, \nu) = \left| \frac{1 - \sqrt{\epsilon(T, \nu)}}{1 + \sqrt{\epsilon(T, \nu)}} \right|^2. \quad (12)$$

This introduces a new parameter, the dielectric constant ϵ_∞ , which is often taken to be unity. In our calculations, we will also set $\Omega_p = 1$ eV.

III. NUMERICAL RESULTS

In Fig. 1(a), we present results for the reflectance ratio $r_s(t, \nu)/r_n(\nu)$ at several reduced temperatures $t = T/T_c$ as labeled. Here, the subscripts s and n stand for superconducting and normal state, respectively. The anisotropy parameter defining the extended s -wave gap $x = 0.67$ ($\alpha = 0.9$) with the critical temperature set at $T_c = 20$ K, zero-temperature gap amplitude $\Delta_0 = 10$ meV, and quasiparticle impurity elastic quasiparticle scattering rate πt^+ , with $t^+ = 1.5$ meV. These values are reasonable for the ferropnictides.^{54,55} The width of the normal-state Drude-type contribution in Refs. 54–57 and 59 is of order 100 cm^{-1} , which is twice the quasiparticle scattering rate. The ratio of gap to T_c value $2\Delta_0/(k_B T_c)$ used here is much larger than in BCS since we wish to model the optical conductivity associated with a large gap amplitude on the electron pocket at point M in the Brillouin zone. For the temperature dependence of $\Delta_0(T)$, we will simply use the classical mean-field BCS temperature dependence

$$\frac{\Delta(T)}{\Delta(0)} = \tanh \left[\frac{T_c}{T} \frac{\Delta(T)}{\Delta(0)} \right]. \quad (13)$$

The (black) short dotted curve is included for comparison and corresponds to a reduced temperature $t = 0.05$ for the case of an isotropic BCS gap (i.e., $x = \alpha = 1$) with all other parameters left unchanged. Note the large differences when compared with the (red) short dashed-dotted curve, which is at the same temperature but includes some gap anisotropy [$x = 0.67$ ($\alpha = 0.9$)]. While the two curves agree well at small energies (ν), they deviate substantially above $\nu \gtrsim 10$ meV. In this region, the anisotropic case begins a rather gradual drop toward one, while the isotropic curve continues to rise slightly before having a precipitous, almost vertical drop to a value below one around $2\Delta_0 = 20$ meV for the impurity content used. At this energy, the (red) short dashed-dotted curve is still above one and is dropping far more gradually. It then has a shallow minimum around $\nu \gtrsim 30$ meV as compared with the minimum in the isotropic curve, which is deeper and occurs at lower energies below $\nu \gtrsim 25$ meV. It is clear from Fig. 1(a) that anisotropy has a significant effect on the shape of the

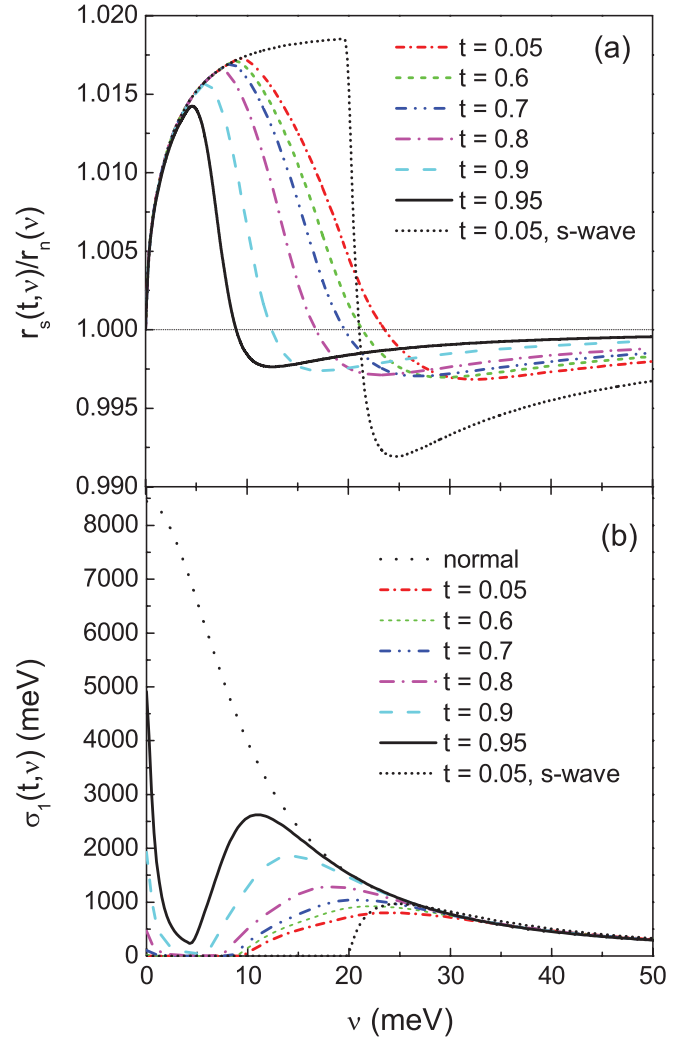


FIG. 1. (Color online) (a) The reflectance ratio $r_s(t, \omega)/r_n(t, \omega)$ between superconducting (s) and normal (n) state as a function of photon energy ν for several values of the reduced temperature $t = T/T_c$ as labeled. The gap anisotropy parameter $x = 0.67$ ($\alpha = 0.9$), $T_c = 20$ K, $\Delta_0 = 10$ meV and the quasiparticle scattering parameter $t^+ = 1.5$ meV. The (black) short dotted curve is for comparison and is for isotropic s wave with the same gap at $t = 0.05$. (b) Gives the real part of the optical conductivity $\sigma_1(t, \nu)$ in meV as a function of ν also in meV. The (black) dotted curve is the corresponding normal-state result and is for comparison. The (black) short dotted curve is for an isotropic s -wave gap and is for comparison.

reflectance ratio. These differences between extended s wave and isotropic s wave become more pronounced when the real part of the optical conductivity $\sigma_1(t, \nu)$ in meV is considered, as it is shown in Fig. 1(b). The (black) dotted curve in this panel is for comparison and describes the normal-state optical conductivity with a Drude width $2\pi t^+ \simeq 9.4$ meV. The (black) short dotted curve is isotropic s -wave BCS at the reduced temperature $t = 0.05$. These two curves agree with the well-known results of Mattis and Bardeen⁵⁸ for absorption through the creation of a hole particle pair out of the condensate. The missing area under the superconducting curve as compared with the normal state goes, of course, into the condensate so that the optical spectral weight is conserved (Ferrell, Glover,

and Tinkham^{69,70} sum rule). The (red) short dashed-dotted curve is to be compared with the isotropic s -wave BCS curve [(black) short dotted] and includes gap anisotropy. We see that anisotropy fills in the region below $2\Delta_0$. Optical absorption now starts already below $\lesssim 10$ meV and this new absorption edge opens much more gradually as compared to the isotropic case, although the impurity scattering rate has not been changed. Also, considerably less optical spectral weight is lost to the condensate. Note that the lower threshold for absorption in the (red) short dashed-dotted curve correlates well with the start of the drop in the reflectance ratio seen in the corresponding curve in Fig. 1(a). It is important here to differentiate between the optical gap ($\Delta_{op}^0 \lesssim 10$ meV here) below which at zero temperature there is no absorption and twice the superconducting gap amplitude Δ_0 , which retains its value of 20 meV. As the temperature is increased toward T_c , the curves for $\sigma_1(t, \nu)$ still show contributions associated with pair-breaking processes out of the condensate, but there is also an additional low-energy Drude-type feature, which comes from direct absorption by thermally excited quasiparticles. A clear kink in the curves allows the two contributions to be identified separately. As T increases, the pair-breaking contribution extends to lower and lower energies and the quasiparticle contribution increases in magnitude.

Returning to the zero-temperature case, we focus on the extra absorption associated with the anisotropic as compared to the isotropic case. We define the remaining optical spectral weight up to $\nu_c = 2\Delta_0$ as

$$A_s = \int_0^{\nu_c} d\omega \sigma_{1s}(T \simeq 0, \omega) \quad (14)$$

and take its ratio with the normal-state value for the same quantity denoted by A_n . This ratio is shown in Fig. 2 as a function of the anisotropy parameter x . For $x = \alpha = 1$, the isotropic case $A_s/A_n = 0$. The optical spectral weight due to anisotropy increases as x decreases because the conductivity becomes finite in the region below 10 meV down to the value of the minimum gap. On the other hand, our numerical

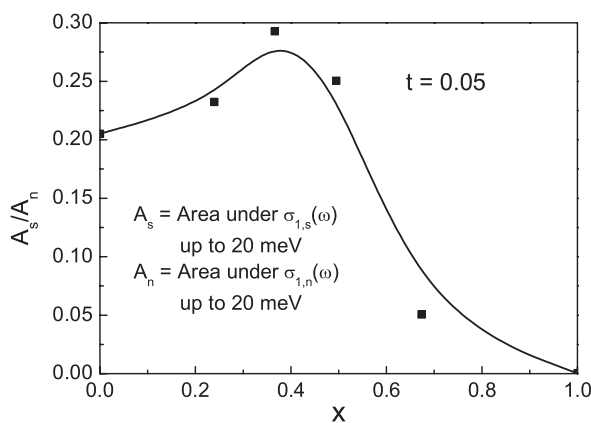


FIG. 2. The ratio of the area under the conductivity in the superconducting state A_s to its normal-state equivalent A_n up to $\nu_c = 2\Delta_0 = 20$ meV [according to Eq. (14)] as a function of the gap anisotropy parameter x . The isotropic s wave corresponds to $x = 1$, while $x = 0$ is a case for which the superconducting gap averages to zero on the Fermi surface.

calculations show that adding a subdominant s -wave part to a pure d -wave gap always increases the ratio A_s/A_n and, thus, this ratio must have a maximum somewhere between $x = 0$ and 1. Here, the maximum of about 0.25 is reached around $x = 0.37$ ($\alpha = 0.55$) before decreasing slightly toward ~ 0.2 at $x = \alpha = 0$. This is the case when the average superconducting gap is zero. These results are in good agreement with the data of Lobo *et al.*⁵⁷ for $\text{BaFe}_{2-x}\text{Co}_x\text{As}_2$. These authors noted that the amount of optical spectral weight remaining in their sample at low temperatures above what would be expected in a single-gap analysis based on Mattis and Bardeen⁵⁸ was of order 25%. This is assigned to anisotropy in the gap on the electron pocket at the M point in the Brillouin zone. We note, however, that this assignment does not provide a strong constraint on the anisotropy parameter x other than that it be of order 0.49 or less ($\alpha \leq 0.7$). At its upper limit, it would fall near the crossover region between a small gap and nodes.

When the optical gap Δ_{op}^0 becomes very small, the energy dependence of the optical conductivity can provide information on whether Δ_{op}^0 is zero or finite, even if its value falls below the lowest probing photon energy. The temperature dependence of $\sigma_1(T, \nu)$ can also provide additional information on this same issue. This is illustrated in Fig. 3, which has two frames. Figure 3(a) is for $x = 0.49$ ($\alpha = 0.7$) and, for the impurity scattering rate considered, ($t^+ = 1.5$ meV) has a small optical gap as revealed in the (red) short dotted curve for the lowest reduced temperature $t = 0.05$. Figure 3(b) is for $x = 0.37$ ($\alpha = 0.5$) and there is a node in this case. The optical conductivity at the same reduced temperature $t = 0.05$ [(red) short dotted curve] has now a completely different behavior. While in Fig. 3(a) there is a region of zero optical conductivity (no absorption) at small ν , now the conductivity in this frequency range remains everywhere of order one quarter its normal-state value shown in both frames as the (black) dotted curve. As the temperature is increased, the optical gap in Fig. 3(a) fills in and there is some absorption at all frequencies, including the appearance of a thermal Drude peak about $\nu = 0$. But, there remains a minimum. An estimate of the optical gap that exists at $T = 0$ can be deduced from the position in energy of the minimum in $\sigma_{1s}(T, \nu)$ versus ν even for the reduced temperature $t = 0.4$ [(cyan) dashed-dotted curves]. At temperatures as high as $t = 0.95$ [solid (black) curves], just below T_c , a signature of the gap formation is still seen as a minimum in $\sigma_{1s}(T, \nu)$ versus ν , although this minimum has moved to higher frequencies on the ν axis as compared to the zero-temperature optical gap. Such a minimum is not seen in Fig. 3(b), where the superconducting gap has nodes. The large difference noted between the case of a small optical gap and no gap allows one to distinguish clearly between the two, even if the probing photon energy is not sufficiently small and the temperature sufficiently low for a region zero conductivity to be revealed. In Fig. 4, we show our results for the reflectance ratio $r_s(t, \nu)/r_n(t, \nu)$ for the same two values of gap anisotropy $x = 0.49$ ($\alpha = 0.7$) [Fig. 4(a)] and $x = 0.37$ ($\alpha = 0.5$) [Fig. 4(b)] as we used in Fig. 3. All other parameters stay unchanged. In this case, the difference between a small gap [Fig. 4(a)] and nodes [Fig. 4(b)] is not as obvious as for the real part of the optical conductivity shown in Fig. 3. The distinguishing feature is that in Fig. 4(a), all curves

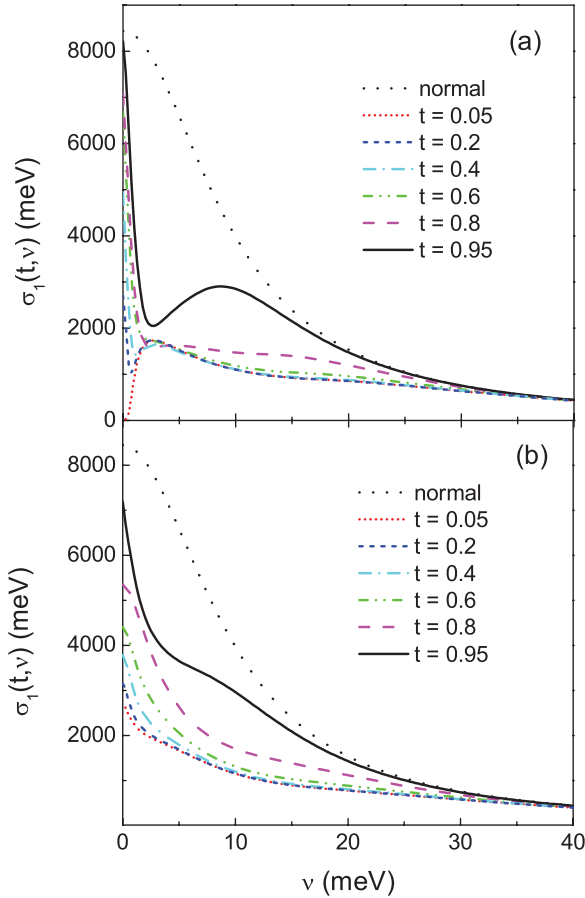


FIG. 3. (Color online) (a) The real part of the optical conductivity $\sigma_1(t, \nu)$ in meV as a function of the photon energy ν in meV for several values of the reduced temperature $t = T/T_c$ as labeled. The gap anisotropy parameter $x = 0.49$ ($\alpha = 0.7$), $T_c = 20$ K, and $\Delta_0 = 10$ meV and the quasiparticle elastic impurity scattering parameter $t^+ = 1.5$ meV. (b) The same as (a) but for $x = 0.37$ ($\alpha = 0.5$). For $x = 0.49$, the system shows a small finite gap at $t = 0.05$, while for $x = 0.37$, the superconducting gap has nodes at the same temperature.

fall below one and approach one from below as ν becomes large, while in Fig. 4(b), the reflectance ratio remains above one at all temperatures and photon energies.

Returning to the real part of the optical conductivity, we show additional results in Fig. 5 for the frequency dependence of the ratio $\sigma_{1s}(\nu)/\sigma_{1n}(\nu)$ as a function of ν in meV and for three different temperatures, namely, $T = 20$ K in Fig. 5(a), $T = 10$ K in Fig. 5(b), and $T = 1.5$ K in Fig. 5(c). In each frame, seven values of gap anisotropy are considered as labeled in the figures. It is described by the parameter x , which when multiplied by 100 gives the percentage of isotropic s wave included in our extended s -wave model. The case $x = 1$ corresponds to the familiar isotropic BCS s wave, while $x = 0$ corresponds to the case when the superconducting gap averages to zero, i.e., it has no isotropic s -wave component. As can be seen in Fig. 5(c), the (green) dashed-dotted curve [$x = 0.44$ ($\alpha = 0.62$)], the (cyan) dashed-double dotted [$x = 0.49$ ($\alpha = 0.7$)], the (magenta) short dashed [$x = 0.67$ ($\alpha = 0.9$)], and (black) short dotted ($x = 1$) curves correspond to cases where there is an optical gap at low temperatures (T) close to

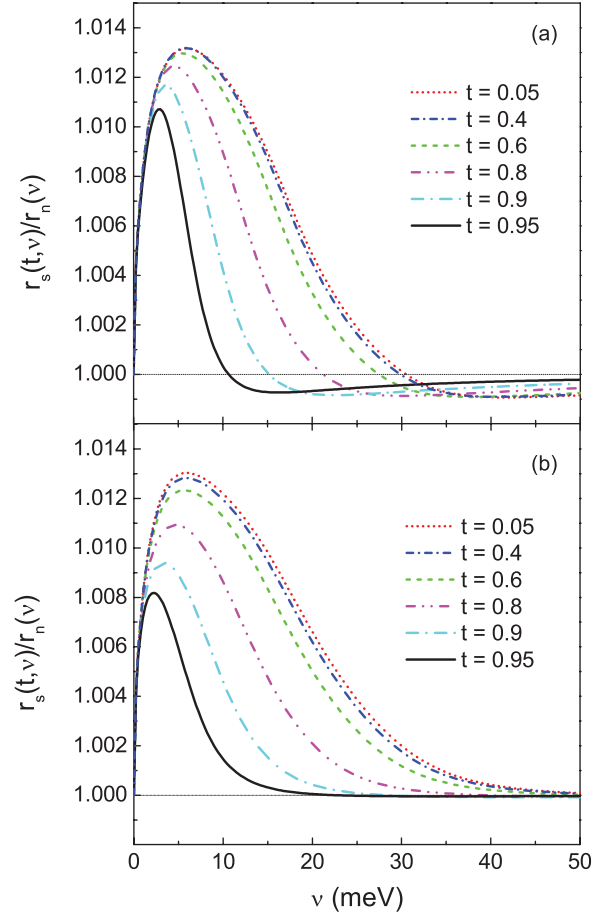


FIG. 4. (Color online) (a) The ratio of superconducting- to normal-state reflectance $r_s(t, \nu)/r_n(\nu)$ vs photon energy ν in meV for several reduced temperatures $t = T/T_c$ as labeled. The gap anisotropy parameter $x = 0.49$ ($\alpha = 0.7$), $T_c = 20$ K, $\Delta_0 = 10$ meV, and the quasiparticle scattering rate parameter $t^+ = 1.5$ meV. (b) The same as (a) but for $x = 0.37$ ($\alpha = 0.5$). For $x = 0.49$, the system shows a small finite gap at $t = 0.05$, while for $x = 0.37$, the superconducting gap has nodes at the same temperature.

zero T , while the remaining three curves correspond to cases when the superconducting gap has nodes, i.e., (blue) dashed curve [$x = 0.37$ ($\alpha = 0.5$)], (red) dotted curve [$x = 0.24$ ($\alpha = 0.3$)], and (black) solid curve ($x = 0$). These last three curves are strikingly different from the previous ones, and these differences allow one to differentiate between cases with or without optical gap. For the parameters used ($T_c = 25$ K, $\Delta_0 = 7.5$ meV, and $t^+ = 2.5$ meV), which are partially motivated by the data of Ref. 54, the renormalized optical conductivity in the region about $\nu = 0$ is of order ~ 0.5 for the last three curves, while in the other curves, $\sigma_{1s}(\nu)$ has a region where it vanishes. The difference between the case with a small optical gap and the case with a node in the superconducting gap function remains visible for $T = 10$ K [Fig. 5(b)] and even for $T = 20$ K [Fig. 5(a)], although temperature smearing makes the distinction not as sharp. Focusing on Fig. 5(b), we note a sharp minimum in the (cyan) dashed-double dotted and (green) dashed-dotted curves indicative of the optical gap, which is not there in the curves for $x < 0.44$ ($\alpha < 0.62$). We conclude from these results that, even if the optical gap is

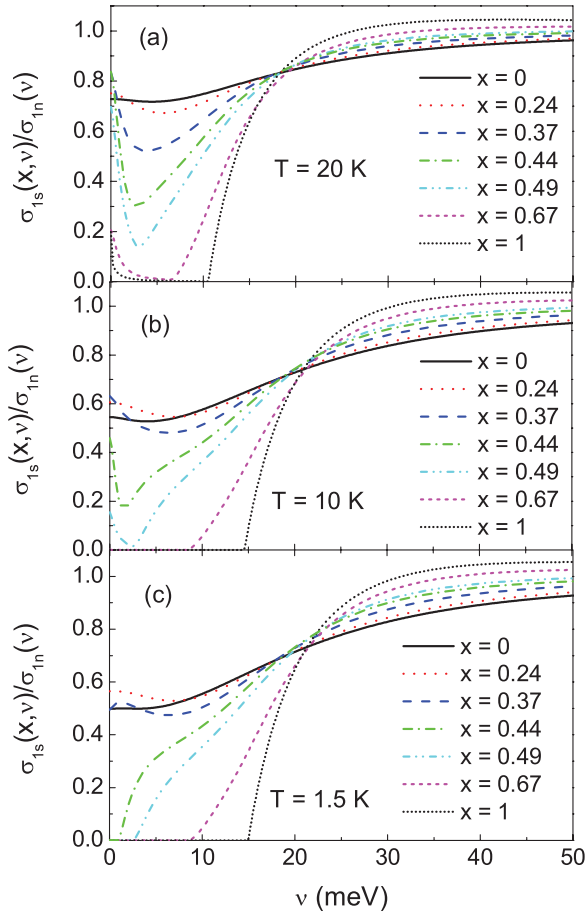


FIG. 5. (Color online) (a) The ratio of the real part of the optical conductivity in the superconducting state $\sigma_{1s}(x, \nu)$ to its normal-state value $\sigma_{1n}(\nu)$ as a function of the photon energy ν in meV for $T = 20$ K. The parameters used are $T_c = 25$ K, $\Delta_0 = 7.5$ meV, and the impurity quasiparticle scattering parameter $t^+ = 2.5$ meV. (b) The same as (a), but for $T = 10$ K. (c) The same as (a), but for $T = 1.5$ K.

smaller than the smallest available photon energy, it is still possible to distinguish between a case with a small optical gap and, thus, a small gap in the quasiparticle DOS and one on the other side of the crossover region with nodes. This remains true even if, in addition, the lowest temperature sampled is a considerable fraction of the critical temperature T_c . We illustrate this with the help of the quasiparticle DOS $N(\omega)/N(0)$, which is shown in Fig. 6 for the same values of x used in Fig. 5 as a function of quasiparticle energy ω . It is given by

$$\frac{N(\omega)}{N(0)} = \left\langle \text{Re} \left\{ \frac{\tilde{\omega}(\omega, \phi)}{\sqrt{\tilde{\omega}^2(\omega) - \tilde{\Delta}^2(\omega, \phi)}} \right\} \right\rangle_{\phi}, \quad (15)$$

where the average is over the polar angle ϕ around the Fermi surface at the M point in the Brillouin zone and $\tilde{\Delta}$, $\tilde{\omega}$ are, respectively, the renormalized superconducting gap function and quasiparticle frequencies at (ω, ϕ) . For the (green) dashed-dotted curve [$x = 0.44$ ($\alpha = 0.62$)], there are no states below $\omega \sim 0.5$ meV, which establishes $\Delta_{qp}^0 \sim 0.5$ meV and, thus, the corresponding optical gap is ~ 1 meV, which is of the same order as the temperature in Fig. 5(b). In

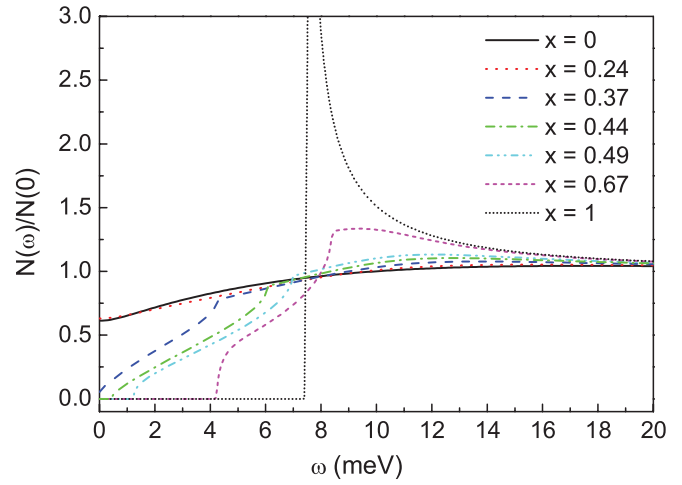


FIG. 6. (Color online) The quasiparticle density of states $N(\omega)/N(0)$ as a function of quasiparticle energy ω in meV. Here, $\Delta_0 = 7.5$ meV and the quasiparticle scattering parameter $t^+ = 2.5$ meV for various values of the anisotropy parameter x as labeled.

contrast, for $x = 0.37$ ($\alpha = 0.5$) [(blue) dashed line], no such gap is observed in the DOS and the superconducting gap function has nodes in this case. Thus, $0.37 \leq x \leq 0.44$ ($0.5 \leq \alpha \leq 0.62$) establishes the crossover region between nodes and a small gap Δ_{qp}^0 . Consequently, when optical gap and temperature are of the same order, there is no region of zero absorption in the optical conductivity, but a deep minimum remains that can, in principle, provide a reliable estimate of the optical gap, which would be revealed more clearly as a zero in $\sigma_{1s}(T, \nu)$ only at much lower temperatures. Even if the optical gap and its corresponding minimum at higher temperatures can not be directly observed, the features described above give a very good indication on which side of the crossover region a particular sample might be.

So far, we considered only a single band. Of course, as we described in the Introduction, a minimum model to capture the physics of the ferropnictides involves two bands, one on the hole pocket around the Γ point (which is believed to be isotropic) and an electron pocket around the M point (which may have a highly anisotropic extended s -wave gap). It is this latter case on which we have concentrated so far. Provided a possible interband contribution is small, we can simply add the conductivities of two independent bands denoted by 1 and 2, respectively, to obtain the total conductivity of the combined system. Charnukha *et al.*⁵³ analyzed optical data in $\text{Ba}_{0.68}\text{K}_{0.32}\text{Fe}_2\text{As}_2$ and found little difference below ~ 30 meV between results with and without including the possibility of an interband contribution. While this contribution is found to increase with photon energy, it is only the region below about twice the maximum gap value that is most relevant. Thus, for our analysis, simply adding the respective conductivities is sufficient. A similar conclusion was also made by van Heumen *et al.*⁵⁹ in $\text{BaFe}_{2-x}\text{Ca}_x\text{As}_2$ for $x = 0.14$. While these authors find interband contributions to start around 10 meV, they remain small in the energy region important for our analysis.

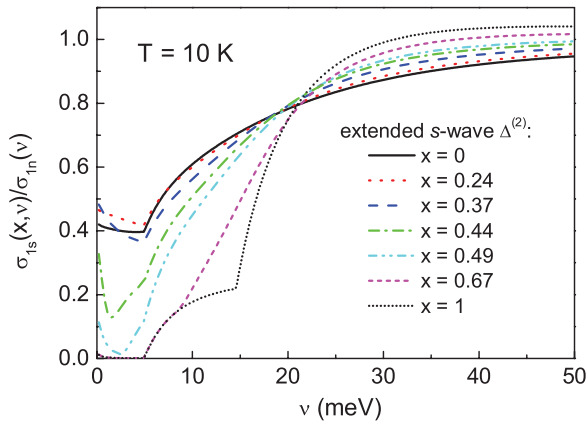


FIG. 7. (Color online) The reduced real part of the optical conductivity $\sigma_{1s}(x, \nu)/\sigma_{1n}(\nu)$ vs photon energy ν in meV for a model with an isotropic s -wave gap function of amplitude $\Delta_0^{(1)} = 2.5$ meV around the Γ point and an extended s -wave symmetry gap function of amplitude $\Delta_0^{(2)} = 7.5$ meV around the M point of the Brillouin zone. The two gap functions contribute 25% and 75%, respectively, to the total conductivity. The results are for $T = 10$ K, $t^+ = 2.5$ meV, $T_c = 25$ K, and various values of the anisotropy parameter x of extended s -wave symmetry gap function as indicated.

In Fig. 7, we show results for the normalized optical conductivity $\sigma_{1s}(x, \nu)/\sigma_{1n}(\nu)$ as a function of photon energy ν for $T = 10$ K in a case when both contributions from the hole band at point Γ and the electron band at point M are included in proportion 25% to 75%, respectively, for illustrative purposes only. It is clear that the characteristic difference in behavior between nodes and the case with a gap Δ_{qp}^0 noted before remains quite detectable in this combined case with an extended s -wave superconducting gap function on the pocket at point M with amplitude $\Delta_0^{(2)} = 7.5$ meV and an isotropic s -wave superconducting gap function on the hole pocket at point Γ with amplitude $\Delta_0^{(1)} = 2.5$ meV. The quasiparticle scattering rate parameter t^+ was set to 2.5 meV on both pockets for simplicity. The crossover region between a small gap Δ_{qp}^0 and nodes falls between $x = 0.44$ ($\alpha = 0.62$) [(green) dashed-dotted curve] and $x = 0.37$ ($\alpha = 0.5$) [(blue) dashed curve] as before in Figs. 5 and 6.

It is clear that the characteristic signature of a single anisotropic extended s -wave gap, which we have emphasized in the main part of this paper, remains clearly visible in the presence of a second isotropic gap. For Fig. 7, this second gap on the hole pocket around the Γ point was taken to be the smaller one of the two, and it shows up as an onset at 5 meV in the (black) short dotted curve. There is a clear second onset at 15 meV corresponding to the second, larger gap, which in the case $x = 1$ is also assumed to be isotropic s wave. As this second gap becomes more anisotropic, i.e., $x < 1$, its minimum value can fall in the region of zero conductivity below 5 meV. This provides finite absorption in this region. It also increases the conductivity in the region of reduced conductivity between 5 and 15 meV because of the hole pocket gap. Should the isotropic gap on the hole band be larger, the first onset of nonzero conductivity at $T = 0$ would become larger, and this would clear the way for an

even sharper picture of the gap anisotropy on the electron pocket.

IV. CONCLUSION

There is evidence that the superconducting gap on the electron pocket around the M point in the Brillouin zone of some ferropnictides is very anisotropic. In the pure limit, there could be nodes in the superconducting gap. Alternatively, a minimum gap Δ_{qp}^0 may exist in the quasiparticle excitation spectrum (or DOS) in all directions on the Fermi surface. In any case, as elastic impurity scattering is increased, the anisotropy will progressively wash out and a new low-energy scale will emerge even when the pure system had nodes. We calculated the optical response of such a superconductor as a function of both photon energy and temperature with particular emphasis on the characteristic signature of the crossover region between nodes and a small minimum gap.

In all cases considered, when there is a node, the ratio of the reflectance in the superconducting state to its normal-state value, never falls below one in contrast to the gapped case for which there is always a region of photon energies where it is less than one and (at large energies) approaches one from below. With nodes, the magnitude of the real part of the optical conductivity at small energies remains at a very significant fraction of its normal-state value of order $\sim 25\%$ even at zero temperature. This can serve as a baseline for comparison with the case when there is a small but nonzero optical gap and the sample falls on the other side of the crossover region between nodes and no nodes. In this case, the real part of the optical conductivity $\sigma_{1s}(T, \nu)$ displays a region of zero absorption if the photon energy ν is below Δ_{op}^0 and the temperature is low enough. But, even at considerably higher values of ν and for temperatures of significant magnitude compared to T_c , the optical conductivity displays a characteristic minimum or a precipitate drop to rather small values, which is not found when there are nodes. We can determine from the position in energy of this minimum that there is an optical gap and provide a good estimate of its actual size. If, on the other hand, the photon energy ν is not low enough to resolve this characteristic minimum, one will not be able to get a good estimate of the size of the optical gap. Nevertheless, the observation of the characteristic precipitate drop of the optical conductivity at low photon energies or the lack thereof will still give a clear indication of which side of the crossover region between nodes and a small gap Δ_{qp}^0 the particular sample is to be placed.

An explicit case of both hole and electron bands demonstrated that the main effects derived for one band remain for two bands, one anisotropic and the other isotropic. For this two-band analysis, we simply add conductivities for hole and electron bands, respectively. There could be an additional contribution from interband transitions, but experiments on $\text{Ba}_{0.68}\text{K}_{0.32}\text{Fe}_2\text{As}_2$ by Charnukha *et al.*⁵³ and on $\text{BaFe}_{2-x}\text{Co}_x\text{As}_2$ for $x = 0.14$ by van Heumen *et al.*⁵⁹ have found this to be small in the low-energy regime most relevant to our analysis of gap symmetry. While, for the hole band around the Γ point, we used isotropic s -wave gap with gap magnitude small compared to the anisotropic gap on the electron pocket around the M point, increasing its size

would create at low energies and $T = 0$ a larger frequency interval of zero conductivity coming from the hole pocket, allowing the anisotropic gap alone to be revealed even more clearly.

ACKNOWLEDGMENT

This research was supported in part by the Natural Sciences and Engineering Research Council of Canada (NSERC) and by the Canadian Institute for Advanced Research (CIFAR).

*schachinger@itp.tu-graz.ac.at

- ¹H. Takahashi, K. Igawa, K. Arii, Y. Kamihara, M. Hirano, and H. Hosono, *Nature (London)* **453**, 376 (2008).
- ²Y. Kamihara, T. Watanabe, M. Hirano, and H. Hosono, *J. Am. Chem. Soc.* **130**, 3296 (2008).
- ³H. Kito, H. Eisaki, and A. Iyo, *J. Phys. Soc. Jpn.* **77**, 063707 (2008).
- ⁴Z.-A. Ren, W. Lu, J. Yang, W. Yi, X.-L. Shen, Z.-C. Li, G.-C. Che, X.-L. Dong, L.-L. Sun, F. Zhou, and Z.-X. Zhao, *Chin. Phys. Lett.* **25**, 2215 (2008).
- ⁵A. S. Sefat, R. Jin, M. A. McGuire, B. C. Sales, D. J. Singh, and D. Mandrus, *Phys. Rev. Lett.* **101**, 117004 (2008).
- ⁶M. Rotter, M. Tegel, and D. Johrendt, *Phys. Rev. Lett.* **101**, 107006 (2008).
- ⁷D. J. Singh and M.-H. Du, *Phys. Rev. Lett.* **100**, 237003 (2008).
- ⁸I. I. Mazin, D. J. Singh, M. D. Johannes, and M.-H. Du, *Phys. Rev. Lett.* **101**, 057003 (2008).
- ⁹L. Boeri, O. V. Dolgov, and A. A. Golubov, *Phys. Rev. Lett.* **101**, 026403 (2008).
- ¹⁰J. Nagamatsu, N. Nakagawa, T. Muranaka, Y. Zenitani, and J. Akimitsu, *Nature (London)* **410**, 63 (2001).
- ¹¹A. A. Golubov, A. Brinkman, O. V. Dolgov, J. Kortus, and O. Jepsen, *Phys. Rev. B* **66**, 054524 (2002).
- ¹²H. J. Choi, D. Roundy, H. Sun, M. L. Cohen, and S. G. Louie, *Nature (London)* **418**, 758 (2002).
- ¹³E. J. Nicol and J. P. Carbotte, *Phys. Rev. B* **71**, 054501 (2005).
- ¹⁴A. V. Chubukov, D. V. Efremov, and I. Eremin, *Phys. Rev. B* **78**, 134512 (2008).
- ¹⁵A. V. Chubukov, M. G. Vavilov, and A. B. Vorontsov, *Phys. Rev. B* **80**, 140515(R) (2009).
- ¹⁶H. K. Leung, J. P. Carbotte, D. W. Taylor, and C. R. Leavens, *Can. J. Phys.* **54**, 1585 (1976).
- ¹⁷H. K. Leung, J. P. Carbotte, and C. R. Leavens, *J. Low Temp. Phys.* **24**, 25 (1976).
- ¹⁸P. G. Tomlinson and J. P. Carbotte, *Phys. Rev. B* **13**, 4738 (1976).
- ¹⁹W. H. Butler, F. J. Pinski, and P. B. Allen, *Phys. Rev. B* **19**, 3708 (1979).
- ²⁰A. A. Abrikosov and L. P. Gor'kov, *Zh. Èks. Teor. Fiz.* **35**, 1558 (1958) [*Sov. Phys. JETP* **8**, 1090 (1959)].
- ²¹E. Schachinger, J. M. Daams, and J. P. Carbotte, *Phys. Rev. B* **22**, 3194 (1980).
- ²²E. Schachinger, M. G. Greeson, and J. P. Carbotte, *Phys. Rev. B* **42**, 406 (1990).
- ²³P. Arberg, M. Mansor, and J. P. Carbotte, *Solid State Commun.* **86**, 671 (1993).
- ²⁴M. Mitrović and J. P. Carbotte, *Can. J. Phys.* **61**, 758 (1983).
- ²⁵M. Mitrović and J. P. Carbotte, *Can. J. Phys.* **61**, 784 (1983).
- ²⁶F. Marsiglio, R. Akis, and J. P. Carbotte, *Phys. Rev. B* **36**, 5245 (1987).
- ²⁷F. Marsiglio, R. Akis, and J. P. Carbotte, *Phys. Rev. B* **45**, 9865 (1992).
- ²⁸E. Schachinger and J. P. Carbotte, *Phys. Rev. B* **62**, 9054 (2000).
- ²⁹B. Mitrović, C. R. Leavens, and J. P. Carbotte, *Phys. Rev. B* **21**, 5048 (1980).
- ³⁰H. Padamsee, J. E. Neighbor, and C. A. Shiffman, *J. Low Temp. Phys.* **12**, 387 (1973).
- ³¹Y. Yanagai, Y. Yamakawa, and Y. Ono, *J. Phys. Soc. Jpn.* **77**, 123701 (2008).
- ³²K. Kuroki, S. Onari, R. Arita, H. Usui, Y. Tanaka, H. Kontani, and H. Aoki, *Phys. Rev. Lett.* **101**, 087004 (2008).
- ³³F. Wang, H. Zhai, Y. Ran, A. Vishwanath, and D.-H. Lee, *Phys. Rev. Lett.* **102**, 047005 (2009).
- ³⁴S. Graser, T. A. Maier, P. J. Hirschfeld, and D. J. Scalapino, *New J. Phys.* **11**, 025016 (2009).
- ³⁵V. Mishra, G. Boyd, S. Graser, T. Maier, P. J. Hirschfeld, and D. J. Scalapino, *Phys. Rev. B* **79**, 094512 (2009).
- ³⁶H. Ding, P. Richard, K. Nakayama, K. Sugawara, T. Arakane, Y. Sekiba, A. Takayama, S. Souma, T. Sato, T. Takahashi, Z. Wang, X. Dai, Z. Fang, G. F. Chen, J. L. Luo, and N. L. Wang, *Europhys. Lett.* **83**, 47001 (2008).
- ³⁷R. Khasanov, D. V. Evtushinsky, A. Amato, H.-H. Klaus, H. Luetkens, C. Niedermayer, B. Büchner, G. L. Sun, C. T. Lin, J. T. Park, D. S. Inosov, and V. Hinkov, *Phys. Rev. Lett.* **102**, 187005 (2009).
- ³⁸D. V. Evtushinsky, D. S. Inosov, V. B. Zabolotnyy, A. Koitzsch, M. Knupfer, B. Büchner, M. S. Viazovska, G. L. Sun, V. Hinkov, A. V. Boris, C. T. Lin, B. Keimer, A. Varykhalov, A. A. Kordyuk, and S. V. Borisenko, *Phys. Rev. B* **79**, 054517 (2009).
- ³⁹A. Koitzsch, D. S. Inosov, D. V. Evtushinsky, V. B. Zabolotnyy, A. A. Kordyuk, A. Kondrat, C. Hess, M. Knupfer, B. Büchner, G. L. Sun, V. Hinkov, C. T. Lin, A. Varykhalov, and S. V. Borisenko, *Phys. Rev. Lett.* **102**, 167001 (2009).
- ⁴⁰V. B. Zabolotnyy, D. S. Inosov, D. V. Evtushinsky, A. Koitzsch, A. A. Kordyuk, G. L. Sun, J. T. Park, D. Haug, V. Hinkov, A. V. Boris, C. T. Lin, M. Knupfer, A. N. Yaresko, B. Buchner, A. Varykhalov, R. Follath, and S. V. Borisenko, *Nature (London)* **457**, 569 (2009).
- ⁴¹C. Liu, T. Kondo, R. M. Fernandes, A. D. Palczewski, E. D. Mun, N. Ni, A. N. Thaler, A. Bostwick, E. Rotenberg, J. Schmalian, S. L. Bud'ko, P. C. Canfield, and A. Kaminski, *Nat. Phys.* **6**, 419 (2010).
- ⁴²Y. Sekiba, S. T., K. Nakayama, K. Terashima, P. Richard, J. H. Bowen, H. Ding, Y.-M. Xu, L. J. Li, G. H. Cao, Z.-A. Xu, and T. Takahashi, *New J. Phys.* **11**, 025020 (2009).
- ⁴³X. G. Luo, M. A. Tanatar, J.-P. Reid, H. Shakeripour, N. Doiron-Leyraud, N. Ni, S. L. Bud'ko, P. C. Canfield, H. Luo, Z. Wang, H.-H. Wen, R. Prozorov, and L. Taillefer, *Phys. Rev. B* **80**, 140503 (2009).
- ⁴⁴M. A. Tanatar, J.-P. Reid, H. Shakeripour, X. G. Luo, N. Doiron-Leyraud, N. Ni, S. L. Bud'ko, P. C. Canfield, R. Prozorov, and L. Taillefer, *Phys. Rev. Lett.* **104**, 067002 (2010).
- ⁴⁵K. Hashimoto, T. Shibauchi, S. Kasahara, K. Ikada, S. Tonegawa, T. Kato, R. Okazaki, C. J. van der Beek, M. Konczykowski,

- H. Takeya, K. Hirata, T. Terashima, and Y. Matsuda, *Phys. Rev. Lett.* **102**, 207001 (2009).
- ⁴⁶E. Schachinger and J. P. Carbotte, *Phys. Rev. B* **80**, 174526 (2009).
- ⁴⁷C. Martin, R. T. Gordon, M. A. Tanatar, H. Kim, N. Ni, S. L. Bud'ko, P. C. Canfield, H. Luo, H. H. Wen, Z. Wang, A. B. Vorontsov, V. G. Kogan, and R. Prozorov, *Phys. Rev. B* **80**, 020501(R) (2009).
- ⁴⁸J. S. Bobowski, J. C. Baglo, J. Day, P. Dosanjh, R. Ofer, B. J. Ramshaw, R. Liang, D. A. Bonn, W. N. Hardy, H. Luo, Z.-S. Wang, L. Fang, and H.-H. Wen, *Phys. Rev. B* **82**, 094520 (2010).
- ⁴⁹B. Muschler, W. Prestel, R. Hackl, T. P. Devereaux, J. G. Analytis, J.-H. Chu, and I. R. Fisher, *Phys. Rev. B* **80**, 180510(R) (2009).
- ⁵⁰J. Yang, D. Hüvonen, U. Nagel, T. Rööm, N. Ni, P. C. Canfield, S. L. Bud'ko, J. P. Carbotte, and T. Timusk, *Phys. Rev. Lett.* **102**, 187003 (2009).
- ⁵¹D. Wu, N. Barišić, M. Dressel, G. H. Cao, Z.-A. Xu, E. Schachinger, and J. P. Carbotte, *Phys. Rev. B* **82**, 144519 (2010).
- ⁵²G. A. Ummarino, M. Tortello, D. Daghero, and R. S. Gonnelli, *Phys. Rev. B* **80**, 172503 (2009).
- ⁵³A. Charnukha, O. V. Dolgov, A. A. Golubov, Y. Matiks, D. L. Sun, C. T. Lin, B. Keimer, and A. V. Boris, e-print arXiv:1103.0938.
- ⁵⁴D. Wu, N. Barišić, M. Dressel, G. H. Cao, Z. A. Xu, J. P. Carbotte, and E. Schachinger, *Phys. Rev. B* **82**, 184527 (2010).
- ⁵⁵N. Barišić, D. Wu, M. Dressel, L. J. Li, G. H. Cao, and Z. A. Xu, *Phys. Rev. B* **82**, 054518 (2010).
- ⁵⁶D. Wu, N. Barišić, P. Kallina, A. Faridian, B. Gorshunov, N. Drichko, L. J. Li, X. Lin, G. H. Cao, Z. A. Xu, N. L. Wang, and M. Dressel, *Phys. Rev. B* **81**, 100512 (2010).
- ⁵⁷R. P. S. M. Lobo, Y. M. Dai, U. Nagel, T. Rööm, J. P. Carbotte, T. Timusk, A. Forget, and D. Colson, *Phys. Rev. B* **82**, 100506 (2010).
- ⁵⁸D. C. Mattis and J. Bardeen, *Phys. Rev.* **111**, 412 (1958).
- ⁵⁹E. van Heumen, Y. Huang, S. de Jong, A. B. Kuzmenko, M. S. Golden, and D. van der Marel, *Europhys. Lett.* **90**, 37005 (2010).
- ⁶⁰T. Fischer, A. V. Pronin, J. Wosnitza, K. Iida, F. Kurth, S. Haindl, L. Schultz, B. Holzapfel, and E. Schachinger, *Phys. Rev. B* **82**, 224507 (2010).
- ⁶¹J. J. Tu, J. Li, W. Liu, A. Punnoose, Y. Gong, Y. H. Ren, L. J. Li, G. H. Cao, Z. A. Xu, and C. C. Homes, *Phys. Rev. B* **82**, 174509 (2010).
- ⁶²M. Nakajima, S. Ishida, K. Kihou, Y. Tomioka, T. Ito, Y. Yoshida, C. H. Lee, H. Kito, A. Iyo, H. Eisaki, K. M. Kojima, and S. Uchida, *Phys. Rev. B* **81**, 104528 (2010).
- ⁶³K. W. Kim, M. Rössle, A. Dubroka, V. K. Malik, T. Wolf, and C. Bernhard, *Phys. Rev. B* **81**, 214508 (2010).
- ⁶⁴J. P. Carbotte and E. Schachinger, *Phys. Rev. B* **81**, 104510 (2010).
- ⁶⁵I. Schürer, E. Schachinger, and J. P. Carbotte, *Phys. C (Amsterdam)* **303**, 287 (1998).
- ⁶⁶E. J. Nicol, J. P. Carbotte, and T. Timusk, *Phys. Rev. B* **43**, 473 (1991).
- ⁶⁷F. Marsiglio, J. P. Carbotte, A. Puchkov, and T. Timusk, *Phys. Rev. B* **53**, 9433 (1996).
- ⁶⁸J. P. Carbotte, C. Jiang, D. N. Basov, and T. Timusk, *Phys. Rev. B* **51**, 11798 (1995).
- ⁶⁹R. A. Ferrell and R. E. Glover, *Phys. Rev.* **109**, 1398 (1958).
- ⁷⁰M. Tinkham and R. A. Ferrell, *Phys. Rev. Lett.* **2**, 331 (1959).